A Linear Motor Launcher System Integrating a Multisurface Superconducting Magnetic Bearing

Sinan Basaran, *Member, IEEE*, Mutlu Altinkilic, and Selim Sivrioglu

***Abstract*—In this article, a linear motor launcher system equipped with superconducting magnetic bearings has been constructed and tested under various conditions. The guide rail of the launcher features permanent magnets that support superconducting levitation and interaction between square prism-shaped bulk superconductors on various surfaces. This results in increased stiffness of a single superconductor along any given axis and comprehensive support of lateral forces. The article investigates the use of a superconducting magnetic bearing in a linear launcher system as a novel approach to a multisurface levitation structure. The experimental system integrates the high-temperature superconductor bulk material-based carriage system and an open cryostat structure. The carriage system levitates on the permanent magnet rail by moving it using an integrated dc linear motor. The article examines the levitation force relationship and performance of the system under different selected speeds and acceleration profiles. The design of the system allows for an adjustable slope of the permanent magnet rail, demonstrating the potential for use as a linear launcher pad. In addition, the proposed system has the potential for application in larger systems, such as maglev vehicles.**

***Index Terms*—Linear launcher system, multisurface levitation, superconducting magnetic bearing.**

I. Introduction

SUPERCONDUCTIVITY and superconducting magnetic levitation are widely used in different areas around the world. Some application areas of superconductivity and superconducting magnetic levitation systems are superconductive magnetic levitation (Maglev) trains, superconducting magnetic bearings [1], [2], [3], [4], superconducting flywheel energy storage systems [5], [6], [7], [8], superconducting electrical machines [9], [10], and superconducting magnetic gears [11], [12]. All these applications are relatively more expensive than their conventional counterparts. Despite their excessive price, in some cases, superconducting applications are preferred over their conventional counterparts. Superconducting magnetic levitation is a technology that utilizes the properties of superconductors and magnetic fields to achieve frictionless and suspended motion. The levitation force is sufficient to support the weight of the superconductor and the object it is carrying, resulting in stable and frictionless levitation. The levitation forces of high-temperature superconductor bulk over a permanent magnet guideway have been reported in some research [13], [14], [15], [16], [17]. All the superconductive applications mentioned here have one thing in common that is due to magnetic levitation, there is no mechanical contact between bodies, which means no mechanical wear due to contact as well as no frictional losses due to rubbing parts. In addition, since there is no need for lubrication between moving bodies, viscous friction can be neglected as well.

Hysteresis is a characteristic of superconductors, and it must be considered in applications such as magnetic levitation systems, where levitation height is important. The complicated hysteresis characteristic in the superconductor has been the subject of various studies [18], [19], [20]. In a permanent magnet (PM) high-temperature superconductor (HTS) pair, the force between HTS and PM is a function of the distance between them. The relation between the distance and the force is not linear, but at very short distances it can be assumed to be linear and using this relation, an equivalent stiffness can be calculated. There are such and similar systems where stiffness and the levitation force of magnetic levitating HTS systems are found experimentally [21], [22].

A superconducting magnetic levitating system can be modeled similarly to a mass damper spring system, where the damper can be substituted with hysteresis and calculated stiffness can be used for the spring constant. Although the modeled system is not perfect and cannot fully reflect the system, for small movements it is acceptable [23].

In superconducting magnetic levitation devices, generally, the interaction on one surface of HTS is studied. In these studies, there is at least one HTS for each axis of motion. However, there are studies where the effect of the magnetic field is studied on the multisurface of HTS [24], [25], [26]. Unlike single-surface HTS, in multisurface studies, a single HTS can be used for different motion axes. Conventional HTS bulk permanent magnet interactions are usually constructed in such a way that only one surface of the superconducting material interacts. The multisurface concept was first proposed by Sivrioglu et al. [25] and involves the placement of permanent magnets on three different surfaces of a ring-shaped superconducting material, resulting

Manuscript received 19 August 2022; revised 21 February 2023 and 12 April 2023; accepted 8 May 2023. Date of publication 12 May 2023; date of current version 6 June 2023. This work was supported by the Scientific and Technological Research Council of Türkiye (TUBITAK) under the support program of 3501 with the project 119M131. This article was recommended by Associate Editor J. M. Pina. *(Corresponding author: Sinan Basaran.)*

Sinan Basaran and Mutlu Altinkilic are with the Department of Mechanical Engineering, Bilecik Seyh Edebali University, 11100 Merkez/Bilecik, Türkey (e-mail: sinan.basaran@bilecik.edu.tr; maltinkilic@gmail.com).

Selim Sivrioglu is with the Department of Mechanical Engineering, Antalya Bilim University, 07190 Döşemealtı/Antalya, Türkey (e-mail: selim.sivrioglu@antalya.edu.tr).

Color versions of one or more figures in this article are available at https://doi.org/10.1109/TASC.2023.3275303.

Digital Object Identifier 10.1109/TASC.2023.3275303

in an increase of 44.25% in the levitation force compared to a single PM-HTS case.

Maglev launcher systems are a potential solution for applications that require high-speed and efficient movement of payloads. They are particularly useful in industrial settings where precision, speed, and accuracy are critical. They can be used in manufacturing facilities for automated material handling and assembly line operations, as well as in distribution centers for sorting and transporting goods. Maglev launchers may also be used in transportation systems, such as high-speed trains, where their smooth and efficient operation can provide a comfortable and efficient mode of travel. In addition, maglev launchers can be used in space launch systems, as a means of efficiently and rapidly launching payloads into space [27], [28], [29]. Maglev launcher systems can be used in various scenarios, including the launching of model aircraft, where speed and acceleration control are important factors. The potential market for these systems includes hobbyists and aeromodelling enthusiasts who are looking for reliable, efficient, and high-performance launch systems. In addition, maglev launcher systems have potential applications in industrial and military settings, such as for the launch of small payloads into space or for launching unmanned aerial vehicles.

In this article, the carriage system formed by using four superconducting bulk materials is levitated on a permanent magnet guide rail produced in accordance with the multisurface method. In addition, unlike the linear magnetic guide rail systems described in the literature, the slope of the designed system can be adjusted mechanically. By incorporating a linear servo dc motor, the carriage system can be moved at various speeds and acceleration profiles. This enables the designed superconducting magnetic levitation system usable as a launching mechanism for unmanned aerial vehicles. In addition, it offers the opportunity to study the real model of the multisurface magnetic levitation system, which can be used in transportation, on a laboratory scale.

The rest of this article is organized as follows. Section II introduces the concept of the multisurface superconducting magnetic bearing, which is used in the linear launcher where the experiments are conducted. Section III shows the experimental studies. Finally, Section IV concludes this article.

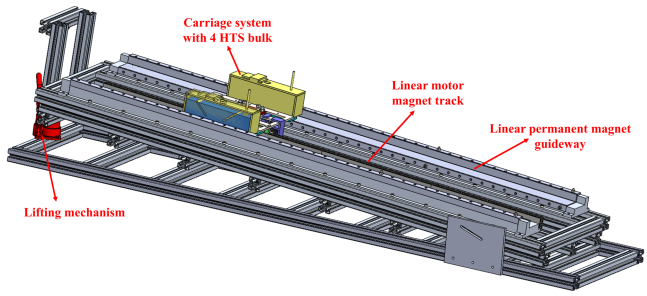

Fig. 1. Illustration of multisurface superconducting magnetic bearing linear motor launcher experimental system.

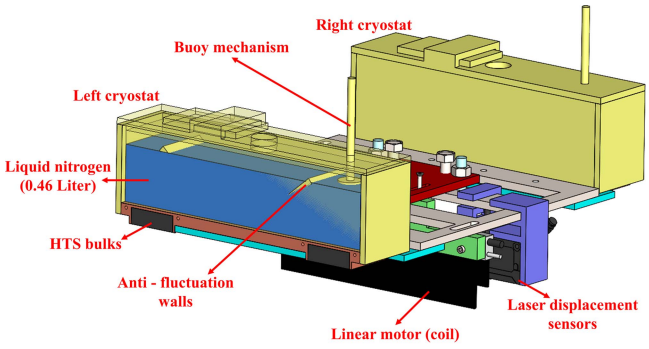

(a)

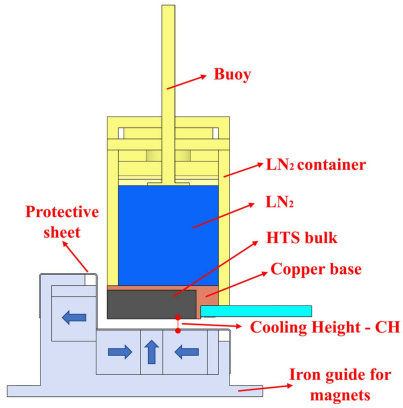

(b)

Fig. 2. (a) Illustration of carriage system. (b) Left cryostat cross-sectional view and permanent magnet guideway.

II. Design of Linear Motor Launcher System

The general view of the designed multisurface superconducting magnetic bearing launcher experimental system is shown in Fig. 1. In this system, a symmetrical multisurface permanent magnet guideway with a total rail length of 1600 mm is positioned on both sides. The platform where guideways are mounted is designed in such a way that its angle can be adjusted with the hydraulic lifting mechanism. A linear dc motor (Omron-R88L-EC-GW-0309) with a servo drive is integrated into the carriage system [see Fig. 2(a)]. In the carriage system, the cryostats on the right and left are symmetrically placed according to the linear motor, which is placed on the same level as the center of mass of the system. Furthermore, the left and right cryostat systems, each with two HTS bulk materials, are mounted at the corners of the carrier system. Fig. 2(b) shows the cross-sectional view of the guideway and left-side cryostat system. The HTS bulk materials used in the cryostat system are single-seed in size of 40 × 40 × 13 mm, supplied from ATZ-GmbH.

The permanent magnet guideway [see Fig. 2(b)] used for multisurface levitation is composed of two different geometries of permanent magnets for the given magnetic orientation. While the dimensions of the permanent magnet used in the middle are 20 × 10 × 20 mm (height × width × depth), the other magnets have a cube geometry of 20 × 20 × 20 mm. In Fig. 2(b), cooling height (CH) represents the height of the mechanical part between the permanent magnet and the superconducting material before levitation begins. Working in different CHs is possible with the system. After the cooling is completed and waiting for a

certain time, the mechanical part is removed, and levitation is achieved. This cooling of superconductors in the system is called the technique of under the magnetic field cooling (FC). Inside the cryostat system, as shown in Fig. 2(b), HTS bulk materials are not in direct contact with liquid nitrogen thanks to the copper block. Nevertheless, due to the high thermal conductivity of copper, the HTS bulk can be cooled to critical temperatures, as if it is in direct contact with liquid nitrogen. Cryogenic conduction paste is applied between the copper plate and the HTS bulk to reduce the contact thermal resistances between the HTS bulk and copper block. Expanded polystyrene foam (EPS) blocks are used as liquid nitrogen containers in the designed open cryostat system. EPS is chosen as the liquid nitrogen container wall material due to its low density and low thermal conductivity. Since it is light in weight, the increase in weight of the carriage due to the container itself is insignificant. Also due to its low thermal conductivity, heat gain by the liquid nitrogen through the walls is reduced. In this design, it is possible to store 0.46 liters of liquid nitrogen in one container. With this amount of stored liquid nitrogen, a levitation time of more than half an hour is achieved. Finally, with a buoy system, it was possible to observe the amount of liquid nitrogen without opening the cryostat filler cap. Four laser noncontact position sensors are employed in the carriage system to measure the displacement in the system while operating at different speeds, or axial displacement under load. Since there was no suitable place for the sensor to be connected to measure the displacement in the center of mass of the carriage, two laser sensors were placed on the front and rear of the carriage, and axial displacement measurements were recorded. Similarly, two laser sensors in the lateral direction are also located at the front and rear of the carriage. The linear dc servo motor provides the movement of the carriage at different speeds and acceleration profiles by getting its position information from the linear absolute optical encoder. The encoder is placed on the ground between the permanent magnet rails. Using this encoder, the motor can be positioned precisely, and it can be controlled with the supervisory control and data acquisition (SCADA) interface thanks to the installed servo drive and programmable logic controller (PLC) system.

A. Cryostat Runtime Test

In the proposed system, cryostats decide the levitation duration of superconductors. The carriage's two cryostats can each hold less than 1 L (≈0.92 L) of liquid nitrogen in total. To measure how long this designed structure can be levitated with stored liquid nitrogen, a long-term displacement measurement experiment was carried out. In the test, it was determined how long the carriage could remain in levitation in the static state by deactivating the linear motor. After the superconductors are cooled to the critical temperature, the carriage begins to levitate, and the recording of measurements starts. Note that after removing the mechanical parts to provide the desired CH, the system makes a certain amount of static displacement. After this point, the displacement value measured from the laser sensors was accepted as zero and the process was started. Fig. 3 shows

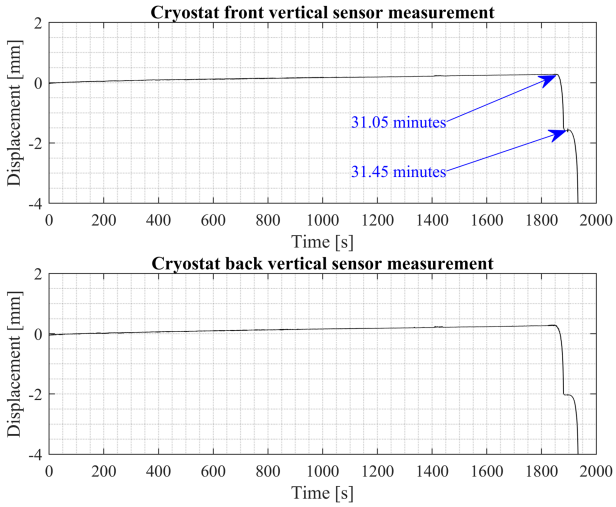

Fig. 3. Cryostat runtime test with displacement measurement.

the displacement measured by the laser sensors placed on the front and back of the carriage. It was observed that levitation continued for a little more than 30 min. The cryostat offers an operation time of over 30 min as an open and noninsulated cryostat structure. As depicted in Fig. 3, two separate decreases are observed at the end of 30 min, at the 31.05 min, and at the 31.45 min. This is because the right and left cryostats are filled in sequence. One cryostat begins to be filled approximately 30 s after the other. Another phenomenon observed in the same way is that the axial displacement increases upward over time. In this case, the amount of liquid nitrogen in containers decreases over time due to evaporation, and the total system weight also decreases over time. Here, the weight of 0.92 L of liquid nitrogen is approximately 0.75 kg.

B. Multisurface Permanent Magnet Guideway Design

For the permanent magnet guideway design, a preliminary study was made for different magnet pole orientations, and the final configuration was selected. The pole orientations of the four permanent magnets used in the design of the permanent magnet guideway are shown in Fig. 4 with arrows. Here, the permanent magnet guideway design corresponding to the lower surface of the HTS bulk, which provides the main lifting force for levitation, was carried out using the Halbach array, which is a well-accepted method. Four possible scenarios for the magnetic pole orientation of the magnet facing the side surface of the HTS have been studied through the analysis, and the scenario with the most uniform vertical and horizontal magnetic flux components has been selected. The magnetic flux density distribution is an important criterion for superconducting magnetic bearings. The magnetic flux density distribution obtained by numerical analysis for permanent magnets of grade N35 is shown in Fig. 4 by considering the bottom and side surfaces of the HTS bulk material on the same graph. Analyses were performed using the COMSOL multiphysics program with the 3-D geometry approach and, stationary magnetic fields (mf) module. The results obtained here are given for a single HTS bulk material. There

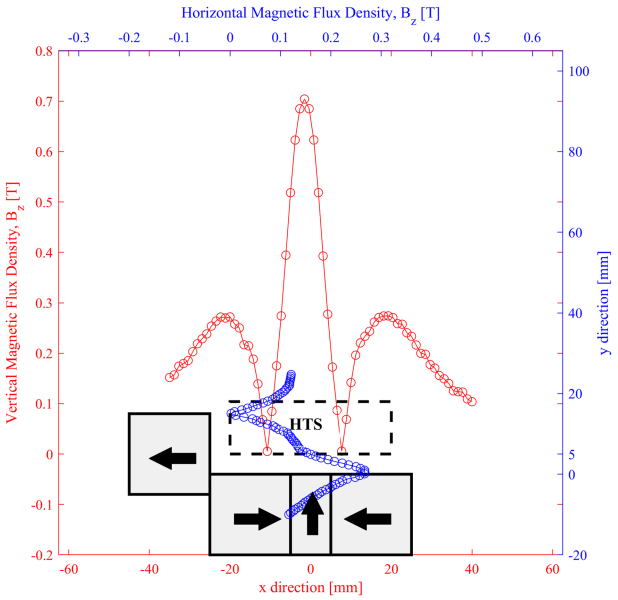

Fig. 4. Vertical and horizontal magnetic flux components.

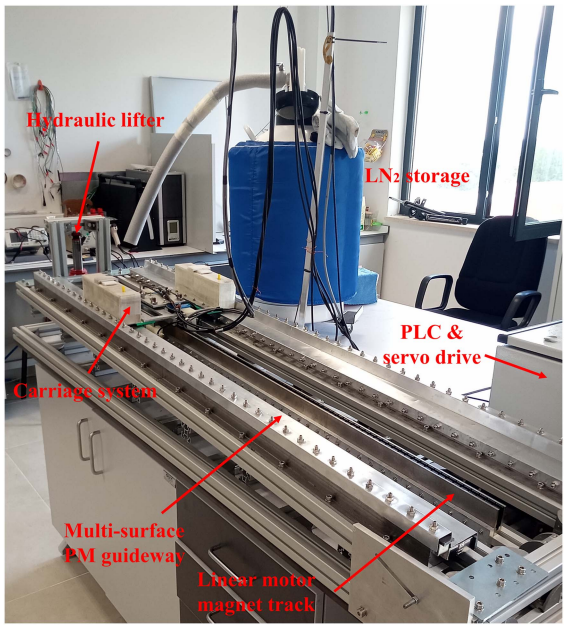

Fig. 5. Experimental setup of multisurface superconducting magnetic bearing linear launcher system.

are a total of four superconductors in the carrier, two on the right and two on the left cryostat.

III. Experimental Studies

The photo of the multisurface superconducting magnetic bearing linear motor launcher system that was developed and built in a research project study is shown in Fig. 5. Using this test setup, experiments can be carried out on the horizontal plane at different speeds, as well as done with inclined planes of different angles. Note that in Fig. 5, this photo was taken, with the system tilted 5 degrees by the hydraulic lift. In addition, a measurable load can be placed on the system, and the force-displacement characteristic of the system can be detected. Experimental studies are grouped into two groups whereas, showing the levitation force of the system and examining the behavior of the system with the selected velocity and acceleration profiles on the inclined surface.

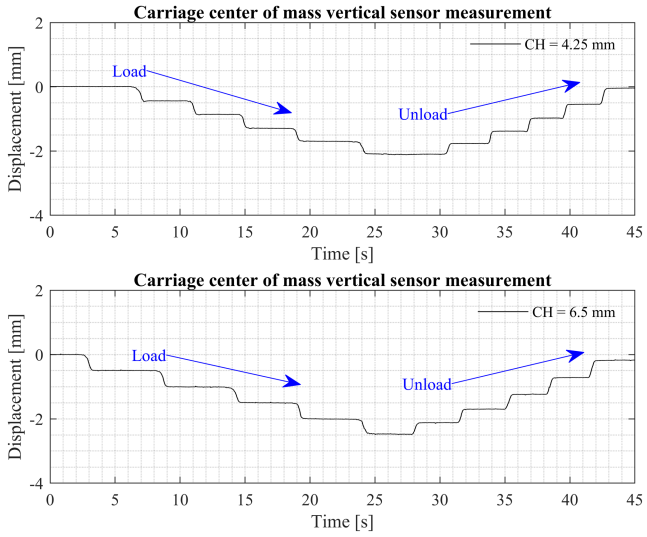

Fig. 6. Time-dependent displacement results under loading and unloading certain masses.

A. Force Characteristics of the Proposed System

Experimental studies were carried out within a certain procedure. The most important characteristic of superconducting magnetic bearings is the force-displacement behavior, which includes the hysteresis effect. First of all, with the technique of under magnetic FC, the carriage system is positioned on permanent magnet guideways with plastic wedges. Note that, at this stage, the connection between the carriage system and the linear motor is disconnected. Then, both cryostats are filled with liquid nitrogen, allowing the HTS bulks to switch into the superconducting phase. After removing the mechanical wedge parts, it is observed that the carriage system performs some downward static displacement. The carriage system was then loaded with five equal weights of 1175 grams and waited for a set period of time. After waiting for a certain time likewise, the loaded weights of equal mass were sequentially unloaded. This procedure was repeated for CH = 4.25 mm and CH = 6.5 mm. The time-dependent displacement results obtained in these experiments are shown in Fig. 6. Blue arrows indicate loading and unloading sequences. In superconductive magnetic levitation systems, a hysteresis effect occurs in the loading and unloading conditions of the system. Although motorized devices with loadcell are needed to see the hysteresis effect, this effect can also be seen in the magnetic levitation system under loading and unloading conditions. Fig. 7 shows the force-displacement curves obtained for two different CHs. As can be seen in Fig. 7, the amount of hysteresis increases as the amount of CH increases.

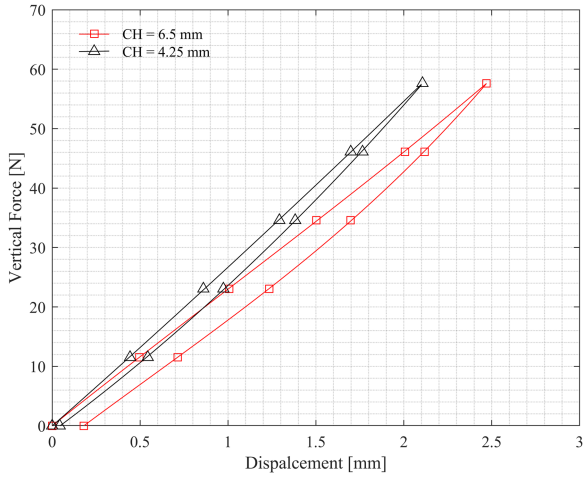

Fig. 7. Variation of levitation force with displacement.

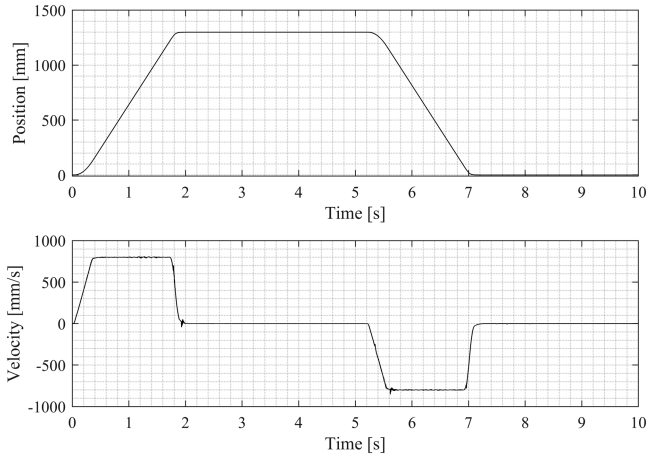

Fig. 8. Position and velocity of the carriage system ($v = 800$ mm/s).

B. Experimental Studies at Different Moving Speeds of the Carriage System

The proposed test system is designed to be a launcher that allows the desired speed, acceleration, and jerk values to be adjusted. Therefore, a PLC interface is created for the linear servo dc motor and is controlled based on SCADA. As a working principle of the linear motor, the position information should instantly be available with precision. Although the designed system length is 1600 mm, the actual stroke distance for the movement of the carriage is 1300 mm due to the carriage width. In the launcher system, position information is obtained by the Fagor absolute optical encoder, which has a reading distance of 1300 mm, and is compatible with the protocol of the dc linear motor. Experimental studies were carried out for two different cases, such as low-speed and high-speed movement of the linear motor launcher system. In the experiments, the carriage system moved from the home position to the end position of 1300 mm, and after a waiting period, it returned back to the home position by making a reverse movement with the same selected speed and acceleration. Fig. 8 shows the position and velocity graphs

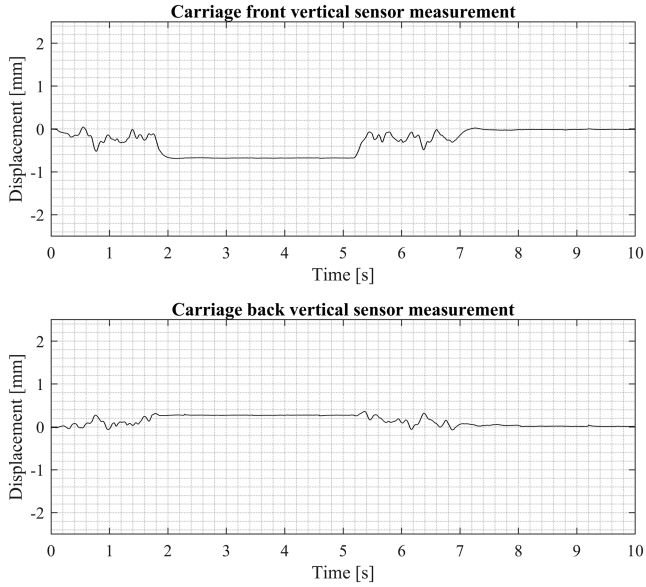

Fig. 9. Vertical displacement of the carriage system ($v = 800$ mm/s).

created with the PLC program for the 800 mm/s carriage speed. The PLC interface is used to save these data. In this profile, 2500 mm/s^2 is selected as the start ramp, and 15 000 mm/s^2 is selected for the stop ramp. In addition, a Jerk value of 100 000 mm/s^3 was applied to the profile. These values were created to demonstrate the usability of the system as a laboratory-scale launcher. Different values can be chosen for the application type of the superconducting levitation system. It should be noted that for maglev transportation systems, the acceleration and jerk values are selected to fall within the acceptable standards of public transportation. Fig. 9 shows the displacements measured by vertical laser displacement sensors positioned at the front and rear of the carriage system when the system is positioned 5° upward. Similarly, the lateral displacements obtained at a speed of 800 mm/s are presented in Fig. 10. The measurements obtained in Figs. 9 and 10 were given for the system at FC = 4.25 mm. When the cooling process was completed and the mechanical wedge parts were removed, the displacement began to be measured using the laser displacement sensors. The speed of the system can be adjusted within the limits of the liner motor via the PLC program. Under the selected ramp and jerk values, the system can reach a maximum speed of 2200 mm/s. The velocity profile and position information used for this velocity value are given in Fig. 11. Vertical and lateral displacement results obtained for 2200 mm/s velocity and CH = 4.25 mm under the same acceleration, jerk, and incline conditions are given in Figs. 12 and 13, respectively. As seen in Figs. 12 and 13, the reason of the vertical displacement sensor output is different from the outputs of the front and rear laser displacement sensors on the carriage system are the pitching behavior of the system during the forward movement. This creates a hysteresis effect in the system. But in the backward movement, it is observed that the vertical position returns to its original state. Lateral displacements are largely due to the gap connection between the linear motor and the carriage system. As a result, it is observed

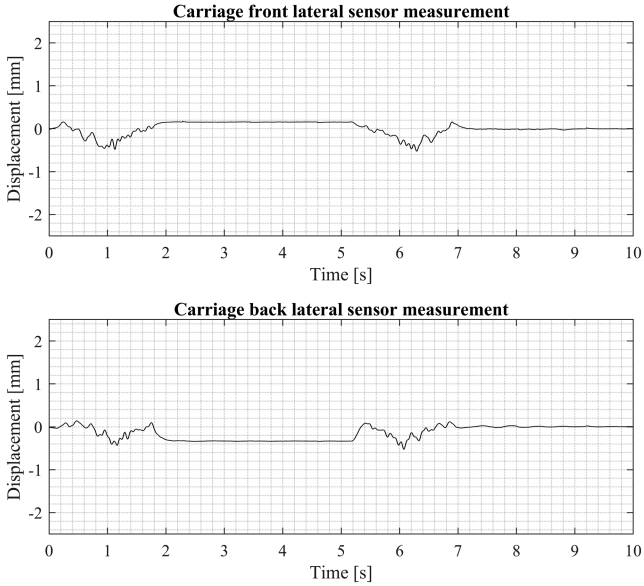

Fig. 10. Lateral displacement of the carriage system ($v = 800$ mm/s).

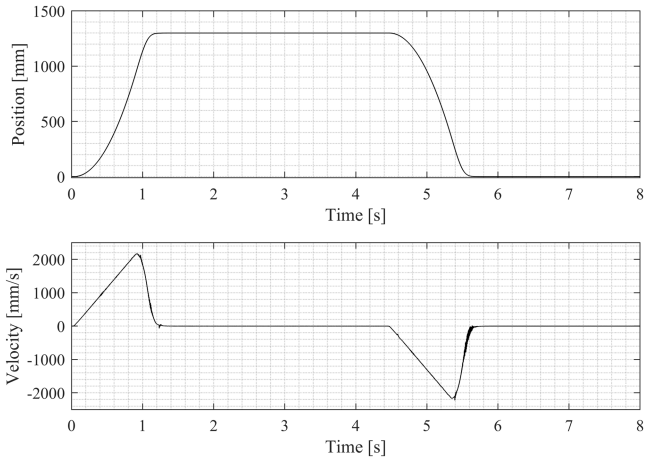

Fig. 11. Position and velocity of the carriage system ($v = 2200$ mm/s).

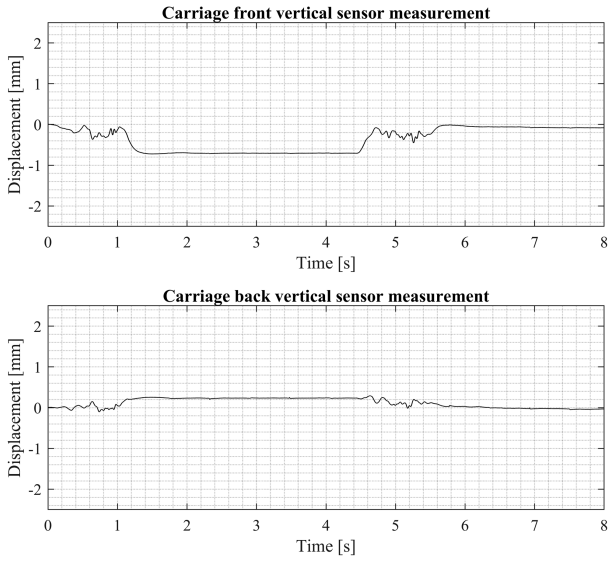

Fig. 12. Vertical displacement of the carriage system ($v = 2200$ mm/s).

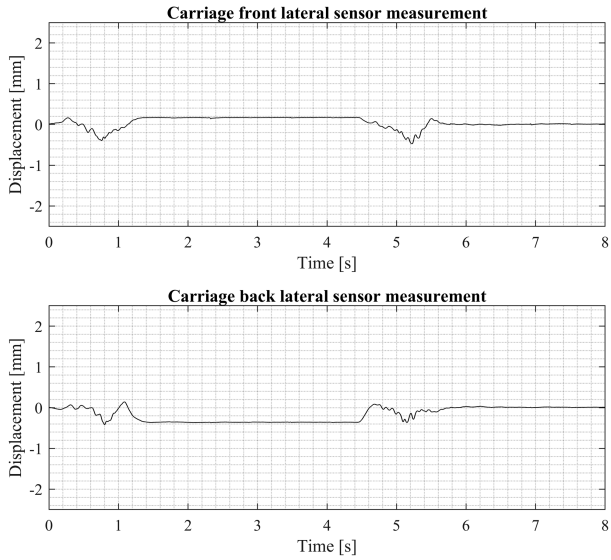

Fig. 13. Lateral displacement of the carriage system ($v = 2200$ mm/s).

that the figures obtained at different speed conditions show the same behavior, but the amplitudes of the displacements begin to decrease with the increase in the system speed. This behavior demonstrates the suitability of superconducting magnetic levitation systems for high-speed maglev transport applications.

IV. Discussions

Launchers used to launch small and medium-sized target unmanned aerial vehicles or model unmanned aerial vehicles are produced as conventional catapult launchers or pneumatic launcher systems. In this type of unmanned small aircraft, the speed and acceleration values during launch are important. In practice, high acceleration values during launch can cause destruction of the launched aircraft. It is quite difficult to control the acceleration in this type of conventional launcher. However, it may take some time to prepare the launcher system for subsequent launches, particularly in pneumatic systems, because filling the tank with the required amount of air extends the preparation time.

One of the aims of this research study is to understand the applicability of the proposed launcher system to practical use. The results obtained in the proposed superconducting bearing linear motor launcher experiments show that speed and acceleration control are possible in the launching of model aircraft. On the other hand, the operation time of cryostats used for cooling superconductors is limited to up to 30 min in this research study. This drawback can be overcome with vacuum-type cryostats that provide cooling for more than 30 h [30].

V. Conclusion

In this article, a laboratory-scale linear motor launcher with a superconducting magnetic bearing is proposed and tested in different speed and acceleration cases. The established superconducting magnetic bearing linear launcher system provides

important information from an engineering point of view. In the established system, first, it is tested for static runtime test. Then, the constant mass payloads are loaded and unloaded, to show the force characteristics of the maglev system. Finally, the motion performance on the inclined rail under various speed and acceleration conditions is investigated. Although the designed system to be a launcher as a concept, it also has the potential to be applied to large-scale systems such as maglev vehicles.

REFERENCES

[1] L. S. Mattos, E. Rodriguez, F. Costa, G. G. Sotelo, R. De Andrade, and R. M. Stephan, "MagLev-cobra operational tests," *IEEE Trans. Appl. Supercond.*, vol. 26, no. 3, Apr. 2016, Art. no. 3600704, doi: 10.1109/TASC.2016.2524473.

[2] R. Tero et al., "Experiments in a real scale Maglev vehicle prototype," *J. Phys. Conf. Ser.*, vol. 234, no. 3, Jun. 2010, Art. no. 032054, doi: 10.1088/1742-6596/234/3/032054.

[3] G. G. Sotelo, R. A. H. De Oliveira, F. S. Costa, D. H. N. Dias, R. De Andrade, and R. M. Stephan, "A full scale superconducting magnetic levitation (MagLev) vehicle operational line," *IEEE Trans. Appl. Supercond.*, vol. 25, no. 3, Jun. 2015, Art. no. 3601005, doi: 10.1109/TASC.2014.2371432.

[4] Z. Deng et al., "A high-temperature superconducting Maglev ring test line developed in Chengdu, China," *IEEE Trans. Appl. Supercond.*, vol. 26, no. 6, Sep. 2016, Art. no. 3602408, doi: 10.1109/TASC.2016.2555921.

[5] K. B. Ma, Y. V. Postrekhin, and W. K. Chu, "Superconductor and magnet levitation devices," *Rev. Sci. Instrum.*, vol. 74, no. 12, Nov. 2003, Art. no. 4989, doi: 10.1063/1.1622973.

[6] J. Tang, Y. Zhang, and J. Fang, "Superconducting levitation styles for superconducting energy storage flywheel," *Proc. IEEE Int. Conf. Mechatron. Autom.*, 2007, pp. 2889–2893, doi: 10.1109/ICMA.2007.4304018.

[7] Y. Yamauchi, N. Uchiyama, E. Suzuki, M. Kubota, M. Fujii, and H. Ohsaki, "Development of 50 kWh-class superconducting flywheel energy storage system," in *Proc. Int. Symp. Power Electron., Elect. Drives, Automat. Motion*, 2006, pp. 484–486, doi: 10.1109/SPEEDAM.2006.1649820.

[8] K. Nagashima, H. Seino, N. Sakai, and M. Murakami, "Superconducting magnetic bearing for a flywheel energy storage system using superconducting coils and bulk superconductors," *Phys. C Supercond.*, vol. 469, no. 15–20, pp. 1244–1249, Oct. 2009, doi: 10.1016/J.PHYSC.2009.05.245.

[9] P. J. Masson and C. A. Luongo, "High power density superconducting motor for all-electric aircraft propulsion," *IEEE Trans. Appl. Supercond.*, vol. 15, no. 2, pp. 2226–2229, Jun. 2005, doi: 10.1109/TASC.2005.849618.

[10] Y. Itoh et al., "High-temperature superconducting motor using Y-Ba-Cu-0 bulk magnets," *Jpn. J. Appl. Phys.*, vol. 34, no. 10, pp. 5574–5578, Oct. 1995, doi: 10.1143/JJAP.34.5574/XML.

[11] F. Lin, R. Qu, and D. Li, "A novel fully superconducting geared machine," *IEEE Trans. Appl. Supercond.*, vol. 26, no. 7, Oct. 2016, Art. no. 5207605, doi: 10.1109/TASC.2016.2594872.

[12] K. Dong, H. Yu, and M. Hu, "Study of an axial-flux modulated superconducting magnetic gear," *IEEE Trans. Appl. Supercond.*, vol. 29, no. 2, Mar. 2019, Art. no. 5000505, doi: 10.1109/TASC.2018.2889640.

[13] S. Wang et al., "The man-loading high-temperature superconducting Maglev test vehicle," *IEEE Trans. Appl. Supercond.*, vol. 13, no. 2, pp. 2134–2137, Jun. 2003, doi: 10.1109/TASC.2003.813017.

[14] Y. G. Guo, J. X. Jin, J. G. Zhu, and H. Y. Lu, "Design and analysis of a prototype linear motor driving system for HTS Maglev transportation," *IEEE Trans. Appl. Supercond.*, vol. 17, no. 2, pp. 2087–2090, Jun. 2007, doi: 10.1109/TASC.2007.898185.

[15] Z. Deng et al., "A high-temperature superconducting Maglev-evacuated tube transport (HTS Maglev-ETT) test system," *IEEE Trans. Appl. Supercond.*, vol. 27, no. 6, Sep. 2017, Art. no. 3602008, doi: 10.1109/TASC.2017.2716842.

[16] H. Li, Z. Deng, L. Jin, J. Li, Y. Li, and J. Zheng, "Lateral motion stability of high-temperature superconducting Maglev systems derived from a nonlinear guidance force hysteretic model," *Supercond. Sci. Technol.*, vol. 31, no. 7, Jun. 2018, Art. no. 075010, doi: 10.1088/1361-6668/AAC860.

[17] G. Lanzara and G. D'Ovidio, "Characterization method of the V-shaped high-temperature superconducting Maglev module for transport system applications," *J. Supercond. Novel Magnetism*, vol. 35, no. 5, pp. 1071–1078, May 2022, doi: https://doi.org/10.1007/s10948-022-06158-z.

[18] F. C. Moon and P.-Z. Chang, *Superconducting Levitation : Applications to Bearings and Magnetic Transportation*. New York, NY, USA: Wiley, 1994, Art. no. 295.

[19] J. R. Hull and A. Cansiz, "Vertical and lateral forces between a permanent magnet and a high-temperature superconductor," *J. Appl. Phys.*, vol. 86, no. 11, Nov. 1999, Art. no. 6396, doi: 10.1063/1.371703.

[20] C. Navau and A. Sanchez, "Stability and hysteretic losses in superconductor–permanent magnet levitation systems," *Phys. C Supercond.*, vol. 372–376, no. 3, pp. 1474–1477, Aug. 2002, doi: 10.1016/S0921-4534(02)01052-3.

[21] J.-S. Wang and S.-Y. Wang, *High Temperature Superconducting Magnetic Levitation*. Berlin, Germany: De Gruyter, 2017.

[22] J. S. Wang, S. Y. Wang, Z. Y. Ren, M. Zhu, H. Jiang, and Q. X. Tang, "Levitation force of a YBaCuO bulk high temperature superconductor over a NdFeB guideway," *IEEE Trans. Appl. Supercond.*, vol. 11, no. 1, pp. 1801–1804, Mar. 2001, doi: 10.1109/77.920136.

[23] S. Sivrioglu and S. Basaran, "A dynamical stiffness evaluation model for a ring-shaped superconductor magnetic bearing system," *IEEE Trans. Appl. Supercond.*, vol. 25, no. 4, Aug. 2015, Art. no. 3601507, doi: 10.1109/TASC.2015.2417680.

[24] S. Basaran and S. Sivrioglu, "Radial stiffness improvement of a flywheel system using multi-surface superconducting levitation," *Supercond. Sci. Technol.*, vol. 30, no. 3, 2017, Art. no. 035008, doi: 10.1088/1361-6668/30/3/035008.

[25] S. Sivrioglu, S. Basaran, and A. S. Yildiz, "Multisurface HTS-PM levitation for a flywheel system," *IEEE Trans. Appl. Supercond.*, vol. 26, no. 8, Dec. 2016, Art. no. 3603206, doi: 10.1109/TASC.2016.2615076.

[26] K. Ozturk, M. Abdioglu, and Z. Karaahmet, "Magnetic force and stiffness performances of Maglev system based on multi–surface arrangements with three-seeded bulk YBaCuO superconductors," *Phys. C Supercond. Appl.*, vol. 578, Nov. 2020, Art. no. 1353739, doi: 10.1016/J.PHYSC.2020.1353739.

[27] W. Yang, Y. Liu, Z. Wen, X. Chen, and Y. Duan, "Dynamic force properties of a high temperature superconducting Maglev test vehicle," *IEEE Trans. Appl. Supercond.*, vol. 18, no. 2, pp. 799–802, Jun. 2008, doi: 10.1109/TASC.2008.920624.

[28] J. H. Schultz et al., "Superconducting magnets for Maglifter launch assist sleds," *IEEE Trans. Appl. Supercond.*, vol. 11, no. 1, pp. 1749–1752, Mar. 2001, doi: 10.1109/77.920122.

[29] L. H. Zheng, X. Q. Li, and A. G. Wang, "Conceptual models of HTS levitation and linear propulsion system," *IEEE Trans. Appl. Supercond.*, vol. 29, no. 2, Mar. 2019, Art. no. 3601005, doi: 10.1109/TASC.2018.2890120.

[30] U. Floegel-Delor et al., "Mobile HTS bulk devices as enabling ton-force technology for Maglev trains," *IEEE Trans. Appl. Supercond.*, vol. 29, no. 5, Aug. 2019, Art. no. 3601705, doi: 10.1109/TASC.2019.2897216.